

000 001 SENSEFLOW: A PHYSICS-INFORMED AND SELF- 002 ENSEMBLING ITERATIVE FRAMEWORK FOR POWER 003 FLOW ESTIMATION 004 005

006 **Anonymous authors**
007 Paper under double-blind review
008
009
010
011

ABSTRACT

013 Power flow estimation plays a vital role in ensuring the stability and reliability of
014 electrical power systems, particularly in the context of growing network complex-
015 ities and renewable energy integration. However, existing studies often fail to ade-
016 quately address the unique characteristics of power systems, such as the sparsity of
017 network connections and the critical importance of the unique Slack node, which
018 poses significant challenges in achieving high-accuracy estimations. In this paper,
019 we present SenseFlow, a novel physics-informed and self-ensembling iterative
020 framework that integrates two main designs, the Physics-informed Power Flow
021 Network (PPFNet) and Self-ensembling Iterative Estimation (SeIter), to carefully
022 address the unique properties of the power system and thereby enhance the power
023 flow estimation. Specifically, SenseFlow enforces the PPFNet to gradually predict
024 high-precision voltage magnitudes and phase angles through the iterative SeIter
025 process. On the one hand, PPFNet employs the Virtual Node Attention and Slack-
026 Gated Feed-Forward modules to facilitate efficient global-local communication
027 in the face of network sparsity and amplify the influence of the Slack node on
028 angle predictions, respectively. On the other hand, SeIter maintains an exponen-
029 tial moving average of PPFNet’s parameters to create an ensemble model that
030 refines power state predictions throughout the iterative fitting process. Experi-
031 mental results demonstrate that SenseFlow outperforms existing methods, providing a
032 promising solution for high-accuracy power flow estimation across diverse grid
033 configurations¹.
034

1 INTRODUCTION

036 Power flow estimation is a crucial task for maintaining the stable and reliable operations of electrical
037 power systems (Mhlanga, 2023; Khaloie et al., 2024). In practical power systems, any disturbance
038 on a single bus can affect the overall balance of the system, necessitating a recalculation of the power
039 flow to preserve stability. This makes power flow estimation not only essential but also highly fre-
040 quent in operational contexts (Ngo et al., 2024). As shown in Figure 1(a), using the IEEE 39-bus
041 system as an example, the network typically consists of three types of buses: multiple PQ (Load Bus)
042 and PV (Generator Bus) nodes, and a single Slack node. The goal is to determine the voltage mag-
043 nitudes and phase angles at each bus, adhering to the fundamental laws of power system dynamics.
044 While traditional methods like Newton-Raphson (da Costa et al., 1999) and Gauss-Seidel (Elta-
045 maly & Elghaffar, 2017) algorithms offer high accuracy, they face key challenges in modern power
046 grids. As power networks grow in scale and complexity, especially with the integration of renew-
047 ables, these mathematical solvers become computationally inefficient, particularly under large con-
048 tingency (*e.g.*, N-K) analyses (Guo et al., 2021). Additionally, their reliance on complete parameters
049 limits their applicability when critical information, such as nodes’ reactive power, is missing or not
050 measurable—an increasingly common issue in real-world scenarios (Hu et al., 2020).

051 In recent years, data-driven approaches, particularly deep learning techniques, have garnered signif-
052 icant attention for enhancing the accuracy and efficiency of power system analysis (Forootan et al.,
053 2022). Among these approaches, Graph Convolutional Networks (GCNs) (Kipf & Welling, 2017)

¹Code and logs are available in the supplementary materials.

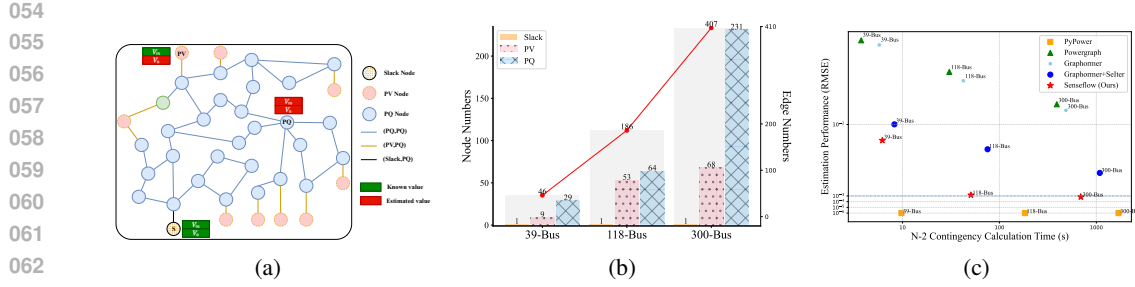


Figure 1: (a) Comparison of the number of nodes and edges across various IEEE standard systems (IEEE 39-Bus, 118-Bus, and 300-Bus), which reveals two key points: 1) there is only one slack node present in each system, and 2) the network exhibits relatively sparse connectivity. (b) Schematic diagram of the IEEE 39-Bus system with typical three different types of nodes and edges. The diagram also shows the parameters to be solved in the power flow calculation, including the phase angle of PV nodes and the voltage and phase angle of PQ nodes, alongside the known values including the voltage and phase angle of the slack node and the voltage of the PV nodes. (c) Tradeoff between the estimation performance on phase angles and the N-2 contingency calculation time.

have emerged as a prominent solution due to their effectiveness in handling graph-structured data, which aligns well with the inherent graph nature of power systems. However, despite their promise, many existing studies (Lin et al., 2024; Ngo et al., 2024; Hu et al., 2020) fall short of fully addressing the unique characteristics of power systems. As depicted in Figure 1(b), one of the key overlooked features is the presence of **only one single slack** bus in any size system, whose phase angle is used as a reference point for the entire system. The Slack bus is also the only node in the system that has both the known voltage magnitude and phase angle. Furthermore, power grids are fundamentally **sparse networks**: the number of edges typically scales linearly with the number of nodes (*i.e.*, $\mathcal{O}(N)$), which is considerably fewer than in fully connected graphs (*i.e.*, $\mathcal{O}(N^2)$). Such sparse connectivity limits information exchange between distant nodes, particularly concerning the Slack node, thereby posing a significant challenge for most GCN architectures that rely on graph connections for efficient node communication. To this end, we aim to employ physic-informed model designs that carefully integrate these distinct features to enhance power flow estimation.

On the other hand, most GCN-based methods follow an end-to-end fitting fashion (Lin et al., 2024; Nellikkath & Chatzivasileiadis, 2022; Falconer & Mones, 2022), which significantly enhances analytical efficiency by directly mapping input graphs to desired flow estimations. As shown in Figure 1(c), while this streamlined process enables rapid power flow analysis, such methods often sacrifice accuracy, as these models may not adequately capture the intricate dependencies and dynamics. In contrast, traditional power flow analysis methods (da Costa et al., 1999; Chang et al., 2007; Trias, 2012) typically employ iterative fitting techniques. These approaches gradually refine their predictions through successive approximations, improving the accuracy of voltage magnitudes and phase angles with each iteration. To this end, we aim to incorporate an iterative process into the GCN-based framework for a refined **tradeoff** between computational efficiency and high precision.

Inspired by these observed limitations, we propose a Physics-Informed and Self-Ensembling Iterative Framework for Power Flow Estimation, dubbed as **SenseFlow**, which seamlessly integrates two novel designs, the Physics-Informed Power Flow Network (PPFNet) and the Self-Ensembling Iterative Estimation (SeIter). **PPFNet** first adopts the Virtual Node Attention (VNA) module to aggregate the features of all nodes into a virtual node and apply cross-attention to distribute global information to individual PQ, PV, and Slack nodes. This facilitates efficient global-local communication without altering the original graph structure, ensuring that each node benefits from system-wide context. We also design the Slack-Gated Feed-Forward (SGF) module in PPFNet to emphasize the Slack node's significance by concatenating its features with PQ and PV nodes. A gated mechanism controls the Slack node's influence, while a residual connection preserves local node characteristics and enhances the Slack node's impact. **SeIter** guides PPFNet to iteratively predict changes in voltage magnitude and phase angle, gradually improving accuracy within each loop. During this process, an exponential moving average (EMA) of PPFNet's parameters maintains an ensemble model that generates more stable outputs, mitigating noise and fluctuations inherent in iterative training. Its

108 outputs are then fed into the next training loop, creating a self-ensembling cycle that progressively
 109 refines the predictions. In each loop, PPFNet is trained using two losses: the ground-truth loss to
 110 align predictions with actual voltage and phase values, and the equation loss to enforce adherence to
 111 power balance equations. Our main contributions are summarized as follows,
 112

- 113 • We propose a novel power flow estimation framework, SenseFlow, which integrates two
 114 novel designs PPFNet and SeIter to obtain high-accuracy power flow estimation iteratively.
- 115 • Our PPFNet carefully addresses the unique characteristics of power systems by designing
 116 the Virtual Node Attention and Slack-Gated Feed-Forward modules, which enhance global-
 117 local communication and optimize the Slack node’s influence effectively.
- 118 • Our SeIter strategy, equipped with a more stable and accurate self-ensembling model, pro-
 119 gressively refines predictions to push the estimation into a high-precision space.
- 120 • Benefiting from the physic-informed design and iterative fitting strategy, our SenseFlow
 121 delivers leading performance in power flow estimation across different-size grid systems.

123 2 RELATED WORK

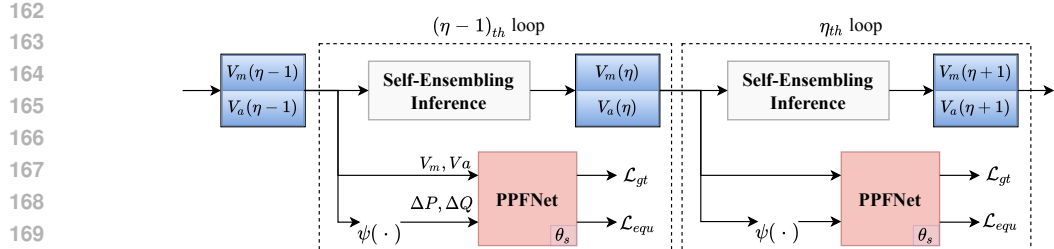
124 Power flow analysis is a fundamental task in electrical power systems that has been extensively re-
 125 searched for decades (Albadi & Volkov, 2020). Traditional methods, such as the Newton-Raphson
 126 Method (da Costa et al., 1999), Gauss-Seidel Method (Eltamaly & Elghaffar, 2017), and Backward-
 127 Forward Sweep (Chang et al., 2007), provide promising estimation accuracy through iterative op-
 128 timization procedures. However, these methods often struggle to scale effectively with larger and
 129 more complex power systems, particularly those incorporating renewable energy sources (Ngo et al.,
 130 2024). Consequently, research groups have increasingly shifted their focus towards data-driven ap-
 131 proaches (Forootan et al., 2022; Khaloie et al., 2024; Goodfellow et al., 2016). Studies along this
 132 line aim to fit the distribution of the collected historical data or simulated data for accurate and
 133 efficient power flow approximation. Considering the collinearity of the training data and the nonlin-
 134 earity of the power flow model, Chen et al. (2021) proposes a piecewise linear regression algorithm
 135 for model fitting. Similarly, Guo et al. (2021) converts the nonlinear relationship of flow calcula-
 136 tion into a higher dimension state space based on the Koopman operator theory. However, most of
 137 these works focused on the nonlinear fitting ability of the model and ignored the graph-structured
 138 topology nature of power systems, leading to unsatisfying estimation performance.
 139

140 Graph Convolutional Networks (GCNs) (Wu et al., 2020; Zhang et al., 2020) are powerful models
 141 designed to handle graph-structured data and have demonstrated significant potential in addressing
 142 the graph topology in power systems (Liao et al., 2021; Falconer & Mones, 2022; Lopez-Garcia
 143 & Domínguez-Navarro, 2023). The work by Owerko et al. (2020) highlights the promising capa-
 144 bility of GCN to leverage the network structure of the data and approximates a specified optimal
 145 solution through an imitation learning framework. Recent studies have incorporated the physical
 146 constraints of power systems into the loss design, enhancing estimation accuracy and robustness to
 147 the variations of typologies (Lin et al., 2024; Gao et al., 2023; Hu et al., 2020). For instance, Habib
 148 et al. (2023) adopts a weakly supervised learning method based on power flow equations, which re-
 149 moves the requirement for labeled data but results in relatively lower accuracy than fully supervised
 150 approaches. PowerFlowNet (Lin et al., 2024) introduces a joint modeling approach that simulta-
 151 neously represents both buses and transmission lines, conceptualizing power flow estimation as a
 152 GNN node-regression problem. However, none of these studies thoroughly examine the distinctive
 153 characteristics of power systems, such as network sparsity and the critical role of the slack node.
 154 Differently, we explore these features and deliberately incorporate them into our network designs.

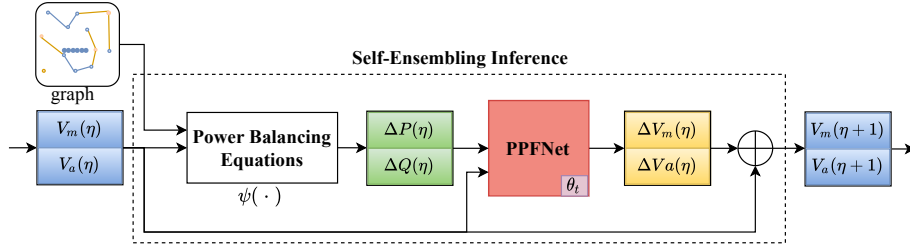
155 3 SENSEFLOW

156 3.1 OVERVIEW

157 Given a power system network \mathcal{G} with N buses (nodes) and E transmission lines (edges), the objec-
 158 tive of power flow estimation is to determine the voltage magnitudes $V_{m,i}$ and phase angles $V_{a,i}$ at
 159 each bus $i \in \{1, 2, \dots, N\}$, subject to the power balance equations that govern active and reactive
 160 power flows in the network. In terms of the training process, we have the active/reactive power for



(a) Iterative power flow estimation



(b) Self-ensembling prediction for the subsequent loop

Figure 2: Illustration of our Self-ensembling Iterative Estimation (SelIter). **(a)** In the η -th loop, the trainable PPFNet (θ_s) receives the input voltage magnitudes $V_m(\eta)$ and phase angles $V_a(\eta)$ from the previous loop and the changes in active and reactive power ΔP and ΔQ calculated by the power balancing equations ψ . The net is trained by two loss functions: the ground-truth loss, \mathcal{L}_{gt} , which aligns the predictions with the actual data, and the equation loss, \mathcal{L}_{equ} , which ensures the model adheres to the physical laws governing the system. **(b)** The Self-Ensembling Inference module prepares the updated data for the next loop. It leverages the self-ensembling teacher model (θ_t) to generate predictions, which serve as the input for the trainable model in the subsequent $\eta + 1$ loop, where θ_t is updated by the exponential moving averaging of θ_s .

PQ nodes, *i.e.*, P^{PQ}/Q^{PQ} , active power P^{PV} and voltage magnitude V_m^{PV} for PV nodes, and known voltage V_m^{Slack} and phase angle V_a^{Slack} for the Slack node, as well as the network topology encoded in the admittance matrix. Giving the ground-truth information on the PQ and PV nodes, including V_m^{PQ} , V_a^{PQ} , V_a^{PV} , our goal is to obtain corresponding accurate predictions.

Our proposed SenseFlow framework addresses the power flow estimation problem by seamlessly integrating physics-informed modeling with a self-ensembling iterative learning process. At its core, SenseFlow leverages both the unique structural features of power systems and the iterative refinement capabilities of ensembling models. Specifically, SenseFlow trains the proposed PPFNet via the SelIter strategy. PPFNet process input data $\mathcal{G}(N, E)$ with known features, P^{PQ}, Q^{PQ} , P_{PV} , V_m^{PV} , V_m^{Slack} , V_a^{Slack} to predict the unknown values on the PV and PQ nodes, *i.e.*, the voltage magnitude \hat{V}_m^{PQ} and phase angle \hat{V}_a^{PQ} for the PQ nodes, and phase angle \hat{V}_a^{PV} for the PV nodes. The training of PPFNet is guided by a ground-truth loss \mathcal{L}_{gt} , and the power balancing equation loss \mathcal{L}_{equ} ,

$$\mathcal{L} = \mathcal{L}_{gt} + \lambda \mathcal{L}_{equ}, \quad (1)$$

where λ is a scalar hyper-parameter to adjust the equation loss weight. Similar to Lopez-Garcia & Domínguez-Navarro (2023); Hu et al. (2020), we use L1 loss for the ground-truth supervision,

$$\mathcal{L}_{gt} = \frac{1}{N_{PQ}} \sum_{i=1}^{N_{PQ}} \left(\left| \hat{V}_{m,i}^{PQ} - V_{m,i}^{PQ} \right| + \left| \hat{V}_{a,i}^{PQ} - V_{a,i}^{PQ} \right| \right) + \frac{1}{N_{PV}} \sum_{j=1}^{N_{PV}} \left| \hat{V}_{a,j}^{PV} - V_{a,j}^{PV} \right|. \quad (2)$$

The power balancing equation loss is applied to encourage minimal power changes,

$$\mathcal{L}_{equ} = \frac{1}{N_{PQ}} \sum_{i=1}^{N_{PQ}} \left(\left| \Delta P_i^{PQ} \right| + \left| \Delta Q_i^{PQ} \right| \right) + \frac{1}{N_{PV}} \sum_{j=1}^{N_{PV}} \left| \Delta P_j^{PV} \right|, \quad (3)$$

216 where the calculations of ΔP and ΔQ are involved in the SeIter process. Through the SeIter strat-
 217 egy, SenseFlow refines its predictions by iteratively updating voltage magnitudes and phase angles.
 218 A self-ensembling mechanism, maintained by exponential moving averages, ensures stability during
 219 the iterative process, progressively pushing the predictions toward higher accuracy. We will detail
 220 these two main designs in the following sections.

222 3.2 SELF-ENSEMBLING ITERATIVE ESTIMATION

224 The self-ensembling iterative estimation (SeIter) diverges from conventional end-to-end learning ap-
 225 proaches. Instead of directly fitting inputs to final voltage magnitudes and phase angles, SeIter gradu-
 226 ally enforces the trainable module to approach the ground truth with the help of a self-ensembling
 227 prediction. As shown in Figure 2(a), the trainable model focuses on fitting the incremental changes
 228 in voltage and phase angle, allowing for refined adjustments with each cycle. This iterative refine-
 229 ment enables the model to achieve accuracy levels that end-to-end approaches may not reach.

230 In the SeIter, each iteration, denoted as the η th loop, involves a dual approach that focuses on both
 231 training the PPFNet model and refining the estimates for voltage magnitude and phase angle for the
 232 future loop. On the one hand, as shown in Figure 2(a), the input data is first utilized to train the
 233 PPFNet, parameterized by θ_s , by minimizing the ground truth loss \mathcal{L}_{gt} . Second, the input data is
 234 subjected to the power balance equations, which yield incremental changes in active power ΔP and
 235 reactive power ΔQ . The objective here is to minimize the equation loss \mathcal{L}_{equ} , which is designed to
 236 ensure that the total power variations approach zero. Let $\psi(V_m, V_a, \mathcal{G})$ denote the Power balancing
 237 equations, the active and reactive power changes ΔP_i and ΔQ_i at the bus i can be calculated by,

$$\Delta P_i = P_i - \sum_{j=1}^N |V_{m,i}| |V_{m,j}| (G_{ij} \cos(V_{a,i} - V_{a,j}) + B_{ij} \sin(V_{a,i} - V_{a,j})), \quad (4)$$

$$\Delta Q_i = Q_i - \sum_{i=1}^N |V_{m,i}| |V_{m,j}| (G_{ij} \sin(V_{a,i} - V_{a,j}) - B_{ij} \cos(V_{a,i} - V_{a,j})), \quad (5)$$

244 where G_{ij} and B_{ij} represent the conductance and susceptance of the line connecting buses i and j .

246 On the other hand, as shown in Figure 2(b), the input data is processed through the Self-Ensembling
 247 Inference module, which maintains an ensembling model, parameterized by θ_t , updated by expo-
 248 nential moving averaging (EMA) of the PPFNet parameters, *i.e.*,

$$\theta_t \leftarrow \alpha \theta_t + (1 - \alpha) \theta_s, \quad (6)$$

251 where α is a common momentum parameter. The ensembling model acts as a stable reference point,
 252 providing an output that reflects the accumulated knowledge from the iterative training process. Its
 253 output is further used as the input for the subsequent iteration, *i.e.*, the $(\eta + 1)$ th loop. This self-
 254 ensembling iterative estimation allows the trainable model to benefit from the progressively refined
 255 outputs of the ensembling model, thereby enhancing its learning capabilities and improving the
 256 overall convergence of the solution.

258 3.3 PHYSICS-INFORMED POWER FLOW NETWORK

260 As shown in Figure 3, our proposed PPFNet is built upon two fundamental modules: the Virtual
 261 Node Attention (VNA) and Slack-Gated Feed-Forward (SGF). VNA enables each node to perceive
 262 global changes without disrupting the underlying graph structure, while SGF enhances the influence
 263 of the slack node on each PQ and PV node, fostering accurate phase angle predictions.

264 *Virtual Node Attention.* Our VNA is specifically designed to address the sparsity issue by providing
 265 each node with the ability to sense and respond to global system variations. This design ensures
 266 that each local node can dynamically adjust its state in response to changes in the overall system,
 267 thus accurately capturing the interdependencies that are essential for maintaining the stability and
 268 reliability of power systems. By incorporating the VNA, we enable a more comprehensive and
 269 adaptive modeling of global interactions, ensuring that the system-wide impact of local changes is
 appropriately reflected. Specifically, We obtain the virtual node representation by contacting all the

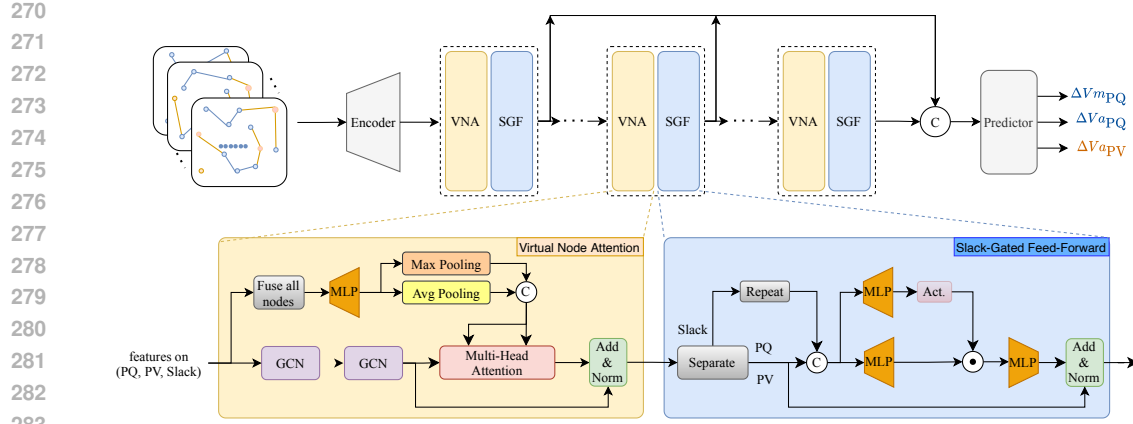


Figure 3: Illustration of our proposed PPFNet, which mainly consists of two main modules, the Virtual Node Attention (VNA) and Slack-Gated Feed-Forward (SGF). The whole hetero-graph is fed into the network. The VNA creates a virtual node by combining and pooling the features of all nodes, then uses cross-attention to selectively communicate global information to each node type. This enhances the interaction between global and local information, preserving the graph structure while improving the model’s ability to capture system-wide dependencies. The SGF combines the slack node’s features with each node’s features through a gated feed-forward network, enhancing the slack node’s influence on other nodes while preserving the original node characteristics via a residual connection. Best viewed on screen.

node features $F_{\text{PQ}}, F_{\text{PV}}, F_{\text{Slack}}$ without breaking the graph structure,

$$F_{\text{afuse}} = \text{Linear}(\text{Concat}(F_{\text{PQ}}, F_{\text{PV}}, F_{\text{Slack}})) \quad (7)$$

$$F_{\text{Vnode}} = \text{Concat}(\text{AvgPool}(F_{\text{afuse}}), \text{MaxPool}(F_{\text{afuse}})) \quad (8)$$

Meanwhile, we can obtain the updated node representation after the graph neural network,

$$F_{\star} = \text{GCN}(F_{\star}), \star \in \{\text{PQ}, \text{PV}, \text{Slack}\} \quad (9)$$

where GCN denotes multi-layer graph convolutional network (*e.g.*, GraphConv (Morris et al., 2019), GAT (Veličković et al., 2018)). Subsequently, we attend the global information to each type of the power node via the cross attention,

$$F_{\star} = \text{LayerNorm}(F_{\star} + \text{softmax} \left(\frac{F_{\star} \cdot F_{\text{Vnode}}^T}{\sqrt{d_k}} \right) F_{\text{Vnode}}) \quad (10)$$

where d_k is the dimension of the F_{Vnode} vectors. In this way, our VNA module preserves the original graph structure and bridges the connection between each node and the whole system without implicitly introducing auxiliary nodes and edges.

Slack-Gated Feed-Forward. Our SGA effectively enhances the influence of the slack node in power system modeling by concatenating its feature representation with the feature representations of each PQ or PV node. The combined features are then processed through a gated feed-forward network, allowing the slack node’s influence to be dynamically adjusted based on the current state of the node. Moreover, a residual connection is added, incorporating the original node features to ensure that local characteristics are preserved while enhancing the model’s ability to accurately capture phase angle relationships throughout the system. Taking the PV node as an example, we have,

$$F_{\text{sfuse}} = \text{Linear}(\text{Concat}(F_{\text{PQ}}, F_{\text{Slack}})) \odot \sigma(\text{Linear}(\text{Concat}(F_{\text{PQ}}, F_{\text{Slack}}))) \quad (11)$$

$$F_{\text{PQ}} = \text{LayerNorm}(F_{\text{PQ}} + \text{Linear}(F_{\text{sfuse}})). \quad (12)$$

To construct the complete model, as shown in Figure 3, we stack K layers of these blocks, allowing for deeper feature extraction and representation learning. In the end, the outputs from all blocks are concatenated and then fed into a predictor module to predict the voltage and phase angles.

324 Table 1: Performance comparison on the IEEE 39-Bus and IEEE 118-Bus system in terms of the root
 325 mean squared error (RMSE), where lower values indicate better performance. “+SeIter” indicates
 326 the application of our proposed self-ensembling iterative estimation process to the corresponding
 327 method. The best results are highlighted in **bold**.

Method	IEEE 39-Bus			IEEE 118-Bus		
	PQ _{Vm}	PQ _{Va}	PV _{Va}	PQ _{Vm}	PQ _{Va}	PV _{Va}
PowerGraph (Varbella et al., 2024)	0.01390720	0.30019834	0.32490083	0.00822813	0.10501729	0.11086510
PowerflowNet (Lin et al., 2024)	0.00700982	0.09310086	0.09836672	0.00188223	0.02760057	0.02899146
TGN (Lopez-Garcia & Domínguez-Navarro, 2023)	0.00489032	0.05125980	0.053372381	0.00138807	0.01697165	0.01895702
GraphConv	0.00724108	0.10125969	0.12637231	0.00192112	0.03769957	0.03597135
GINEConv	0.00768264	0.10450818	0.12893821	0.00194470	0.03934504	0.03760612
SageConv	0.00755344	0.10445687	0.12901593	0.00192444	0.04449241	0.04275129
ResGatedGraphConv	0.00694495	0.10085707	0.12677170	0.00130103	0.03659180	0.03513782
GatConv	0.00808900	0.10591513	0.13207403	0.00262339	0.04434326	0.04388360
TransformerConv	0.00722702	0.10429660	0.13010464	0.00147067	0.04356860	0.04153621
FlowNet (ours)	0.00453724	0.04653547	0.05373371	0.00115526	0.01273561	0.01269017
+ Selter (<i>i.e.</i> , SenseFlow)	0.00078161	0.00608600	0.00609802	0.00009817	0.00102664	0.00103545

4 EXPERIMENT

4.1 DATASETS

We construct our dataset based on standard IEEE test cases (39-Bus, 118-Bus, and 300-Bus) using Matpower (Zimmerman et al., 2010), following approaches similar to Lopez-Garcia & Domínguez-Navarro (2023) and Gao et al. (2023). To simulate diverse scenarios, we introduce variations in power injections, branch characteristics, and grid topology. Specifically, we apply uniform noise to the active and reactive power loads (P and Q), adjusting them to range between 50% and 150% of their original values. Likewise, branch features are perturbed with uniform noise, ranging from 90% to 110% of their baseline values. To examine different grid topologies, we randomly disconnect one or two transmission lines in each sample. All load bus voltage magnitudes are initialized at 1 PU., and phase angles are set relative to the slack bus reference angle. In this way, we generate 100,000 samples for the 39-Bus and 118-Bus systems, and 500,000 samples for the 300-Bus system. 20% of the records are reserved as test sets, with strictly distinct grid topologies from the training data.

4.2 IMPLEMENTATION DETAILS

In our experiments, we utilized a batch size of 256 and employed the Adam optimizer with a learning rate set at 0.001, which follows a cosine decay schedule down to 1e-5 over a total of 100 epochs. Regarding feature embedding sizes, we set them to 128 for the IEEE 39-Bus and 118-Bus systems, while a size of 256 was used for the IEEE 300-Bus system. To effectively integrate information, we stacked a block that combines Virtual Node Attention and Slack-Gated Feed-Forward modules a total of four times. Our models are trained and inferred using an iterative fitting approach with 8 loops to enhance the estimation accuracy. All code was implemented in PyTorch 2.1, and both training and testing were conducted on the 40GB A100 GPU.

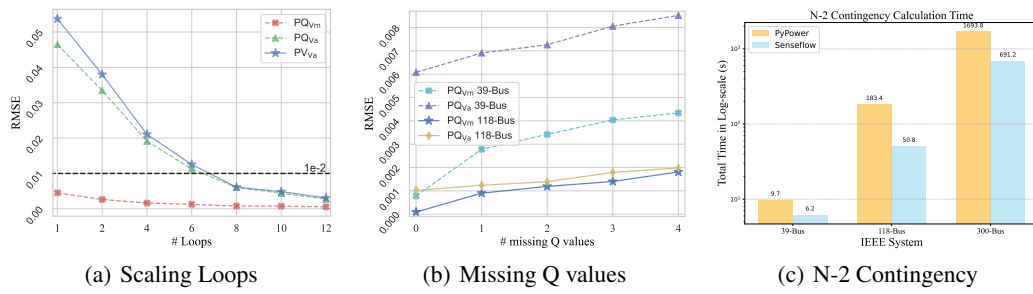
We evaluated our approach against recent studies like Powergraph (Varbella et al., 2024) (with the best transformer-based solution), PowerFlowNet (Lin et al., 2024), and TGN (Lopez-Garcia & Domínguez-Navarro, 2023), and also popular graph networks commonly used in power system analysis, including GraphConv, GINEConv, SageConv, ResGatedGraphConv, GatConv, and TransformerConv. The metrics for comparison focused on the root mean square error of voltage and phase angle predictions for PQ nodes, as well as phase angle predictions for PV nodes.

4.3 ESTIMATION PERFORMANCE

Table 1 presents a performance comparison between our proposed method, SenseFlow (comprising PPFNet and Selter), and other advanced approaches on the IEEE 39-Bus and IEEE 118-Bus systems. The results demonstrate that SenseFlow significantly outperforms the other methods across both systems. In the IEEE 39-Bus system, SenseFlow achieves the lowest root mean square error (RMSE)

378 Table 2: Performance comparison on IEEE 300-Bus system. All notations are the same as in Table 1.
379

380 Method	w/o SeIter			w/ SeIter			Param.
	381 PQ _{Vm}	PQ _{Va}	PV _{Va}	382 PQ _{Vm}	PQ _{Va}	PV _{Va}	
383 GraphConv	0.00088801	0.01430215	0.01519640	0.00018706	0.00177910	0.00158296	8.422M
384 GINEConv	0.00086362	0.01507135	0.01591485	0.00022936	0.00213723	0.00190035	4.227M
385 SageConv	0.00091070	0.01600684	0.01706942	0.00025046	0.00243048	0.00223354	8.422M
386 ResGatedGraphConv	0.00051189	0.01318974	0.01419000	0.00013985	0.00147823	0.00124201	17.105M
387 GatConv	0.00291205	0.01372243	0.02828574	0.00039533	0.00292789	0.00362555	34.112M
388 TransformerConv	0.00053179	0.01439258	0.01582433	0.00016199	0.00206462	0.00216299	55.083M
389 SenseFlow (ours)	0.00093000	0.00417808	0.00473750	0.00010600	0.00086501	0.00077378	21.844M

400 Figure 4: (a) we examine the impact of the iterative loop on the IEEE 39-Bus system. The number
401 of iterations is set to 8 by default, considering the increased inference effort with larger loops. (b)
402 we investigate the missing Q values settings on IEEE 39-Bus and 118-Bus. These settings, without
403 complete known information, cannot be addressed by conventional calculation methods. (c) we
404 compare the total calculation time of N-2 contingency analysis on IEEE standards.
405

406
407 for voltage predictions at PQ and PV nodes, with magnitude error at 0.0007816 and phase angle
408 errors at 0.00608600 and 0.00609802, showcasing its high-precision predictive capabilities. In the
409 IEEE 118-Bus system, SenseFlow also exhibits exceptional performance. While it may not be
410 the absolute best for magnitude predictions of PQ nodes, it remains very competitive and shows
411 remarkable superiority in the more challenging phase angle predictions compared to other methods.
412 Overall, the combination of the PPFNet architecture and the SeIter strategy positions SenseFlow as
413 a highly effective approach for power system state estimation.

414 We investigate the estimation performance of our SenseFlow on the more complex and larger IEEE
415 300-Bus system in Table 2. We can clearly observe that our SenseFlow with SeIter can obtain the
416 state-of-the-art (SOTA) performance, evidenced by consistently lower RMSE values across different
417 metrics. In the absence of our SeIter strategy, we achieved a significant reduction in phase angle
418 prediction error from approximately 0.013 to around 0.004 compared to the second-best method,
419 ResGatedGraphConv. When SeIter is incorporated, SenseFlow emerges as the only method capable
420 of reducing phase angle errors below 1e-3, showcasing its superior performance in this context.
421 These improvements highlight the effectiveness of our method in handling complex power system
422 scenarios and underscore its potential for real-world applications.

423 We reproduce recent studies like Powergraph on our more challenging datasets with larger pertur-
424 bations and varying topologies, and find they fail to handle such settings. Notably, our method
425 performs increasingly better on large 118 and 300-bus systems, since our test sets are built from N-
426 2/3 topology perturbations on IEEE systems, which affect the 39-bus most and make it the hardest.
427

428 4.4 ABLATION STUDY 429

430 *Impact of different components of SenseFlow.* The ablation studies in the Table 3 demonstrate the
431 effectiveness of the key components in our SenseFlow, including the self-ensembling iterative esti-
432 mation (SelIter), block fusion, Virtual Node Attention (VNA), and Slack-Gated Feed-Forward (SGF).

432 Table 3: Ablation studies on our SenseFlow. We examine the effectiveness of the self-ensembling
 433 iterative estimation process (SeIter) and the main components of our proposed FlowNet, including
 434 the block fusion, Virtual Node Attention (VNA) and Slack-Gated Feed-Forward (SGF). Results are
 435 reported on the IEEE 39-Bus. Improvements over the baseline are marked in **blue**.

SeIter	FlowNet				RMSE ↓		
	Base	Fusion	VNA	SGF	PQ _{Vm}	PQ _{Va}	PV _{Va}
	✓				0.00914456	0.12542769	0.14066372 (0.0)
	✓	✓			0.00774126	0.10663362	0.12872563 (↓ 0.01193809)
	✓	✓	✓		0.00561620	0.05007443	0.05717816 (↓ 0.08348556)
	✓	✓		✓	0.00658822	0.07125929	0.07577518 (↓ 0.06488854)
	✓	✓	✓	✓	0.00453724	0.04653547	0.05373371 (↓ 0.08693001)
	✓	✓			0.00102207	0.01159813	0.01238586 (0.0)
	✓	✓	✓		0.00112893	0.01129249	0.01206334 (↓ 0.00032252)
	✓	✓	✓	✓	0.00098343	0.00697184	0.00771528 (↓ 0.00467058)
	✓	✓	✓		0.00100311	0.01011067	0.01089543 (↓ 0.00149043)
	✓	✓	✓	✓	0.00078161	0.00608600	0.00609802 (↓ 0.00628784)

449 Without the SeIter process, introducing the Fusion, VNA, and SGF results in RMSE reductions of
 450 0.01193809, 0.08348556, and 0.06488854, respectively, for the phase angle predictions of PV nodes
 451 compared to the baseline. When these components are combined, forming the complete PPFNet, the
 452 RMSE is further reduced to 0.0537, an overall improvement of 0.0869. More notably, the addition
 453 of SeIter (with a default loop count of 8) significantly decreases all RMSE metrics by approximately
 454 10-fold. As a result, our complete SenseFlow achieves an RMSE of less than 1e-3 for the voltage
 455 magnitude estimation and less than 1e-2 for the phase angle estimation, demonstrating its substantial
 456 improvements and overall effectiveness.

457 *Scaling iterative loops.* Figure 4(a) investigate the effect of scaling iterative loops on the estimation
 458 performance. Specifically, transitioning from a single loop to multiple loops significantly enhances
 459 the accuracy of voltage magnitude and phase angle predictions, with up to 12 loops reducing the
 460 phase angle error by nearly two orders of magnitude. As the number of loops increases, prediction
 461 errors continue to decrease, highlighting the benefits of iterative refinement. However, this
 462 improvement comes at the cost of increased training and inference costs. To balance accuracy and
 463 computational efficiency, we adopt 8 loops as the default, which ensures a phase angle prediction
 464 error below 1e-2 while minimizing computational overhead.

465 *Comparison with mathematical methods. Calculation time.* We compare the total time required
 466 to perform full N-2 contingency simulations on three IEEE test systems using PyPower (a traditional
 467 solver) and our Senseflow (on single GPU-A100-40G). While performance is similar for
 468 small systems, as shown in Figure 4(c), Senseflow achieves 3–5 speedup on larger networks. This
 469 demonstrates the model’s superior scalability for high-volume, large-scale contingency analysis.

470 **Estimation with incomplete inputs.** SenseFlow is capable of accurately estimating voltage states
 471 with missing parameters, a challenge that conventional methods cannot address due to incomplete
 472 information. As shown in Figure 4(b), with missing inactive power in PQ nodes, our method still
 473 achieves estimation performance at the 10^{-3} level, even when more than 10% of PQ nodes lack Q-
 474 values on the 39-Bus system. Compared with TransformerConv and GatConv (Table 1), SenseFlow
 475 achieves lower errors on the 118-Bus system even with Q-value missing.

477 5 CONCLUSION

479 In this paper, we emphasize the importance of the unique features of power systems for power flow
 480 analysis, specifically the sole phase angle-referencing Slack node and the sparse network structure.
 481 To this end, we propose SenseFlow, a novel Physics-Informed and Self-Ensembling Iterative Frame-
 482 work for power flow estimation. By integrating the proposed PPFNet and SeIter strategy, SenseFlow
 483 effectively addresses these characteristics and further enhances the prediction accuracy of voltage
 484 magnitudes and phase angles through iterative refinement. Experimental results demonstrate that our
 485 SenseFlow achieves leading performance in power flow estimation, and extensive ablation studies
 validate the effectiveness of the proposed components and strategies.

486 REFERENCES
487

488 Mohammed Albadi and K Volkov. Power flow analysis. *Computational Models in Engineering*, pp.
489 67–88, 2020.

490 GW Chang, SY Chu, and HL Wang. An improved backward/forward sweep load flow algorithm for
491 radial distribution systems. *IEEE Transactions on power systems*, 22(2):882–884, 2007.

492

493 Jiaqi Chen, Wenchuan Wu, and Line A Roald. Data-driven piecewise linearization for distribution
494 three-phase stochastic power flow. *IEEE Transactions on Smart Grid*, 13(2):1035–1048, 2021.

495

496 Vander Menengoy da Costa, Nelson Martins, and Jose Luiz R Pereira. Developments in the new-
497 ton raphson power flow formulation based on current injections. *IEEE Transactions on power
498 systems*, 14(4):1320–1326, 1999.

499

500 Ali M Eltamaly and Amer Nasr A Elghaffar. Load flow analysis by gauss-seidel method; a survey.
500 *Int J Mech Electr Comput Technol (IJMEC), PISSN*, pp. 2411–6173, 2017.

501

502 Thomas Falconer and Letif Mones. Leveraging power grid topology in machine learning assisted
503 optimal power flow. *IEEE Transactions on Power Systems*, 38(3):2234–2246, 2022.

504

505 Mohammad Mahdi Forootan, Iman Larki, Rahim Zahedi, and Abolfazl Ahmadi. Machine learning
506 and deep learning in energy systems: A review. *Sustainability*, 14(8):4832, 2022.

507

508 Maosheng Gao, Juan Yu, Zhifang Yang, and Junbo Zhao. Physics embedded graph convolution
509 neural network for power flow calculation considering uncertain injections and topology. *IEEE
transactions on neural networks and learning systems*, 2023.

510

511 Ian Goodfellow, Yoshua Bengio, Aaron Courville, and Yoshua Bengio. *Deep learning*, volume 1.
511 MIT Press, 2016.

512

513 Li Guo, Yuxuan Zhang, Xialin Li, Zhongguan Wang, Yixin Liu, Linquan Bai, and Chengshan Wang.
514 Data-driven power flow calculation method: A lifting dimension linear regression approach. *IEEE
Transactions on Power Systems*, 37(3):1798–1808, 2021.

515

516 Benjamin Habib, Elvin Isufi, Ward van Breda, Arjen Jongepier, and Jochen L Cremer. Deep statis-
517 tical solver for distribution system state estimation. *IEEE Transactions on Power Systems*, 2023.

518

519 Xinyue Hu, Haoji Hu, Saurabh Verma, and Zhi-Li Zhang. Physics-guided deep neural networks for
520 power flow analysis. *IEEE Transactions on Power Systems*, 36(3):2082–2092, 2020.

521

522 Hooman Khaloie, Mihaly Dolanyi, Jean-Francois Toubeau, and François Vallée. Review of machine
523 learning techniques for optimal power flow. *Available at SSRN 4681955*, 2024.

524

525 Thomas N Kipf and Max Welling. Semi-supervised classification with graph convolutional net-
526 works. In *International Conference on Learning Representations (ICLR)*, 2017.

527

528 Wenlong Liao, Birgitte Bak-Jensen, Jayakrishnan Radhakrishna Pillai, Yuelong Wang, and Yusen
529 Wang. A review of graph neural networks and their applications in power systems. *Journal of
Modern Power Systems and Clean Energy*, 10(2):345–360, 2021.

530

531 Nan Lin, Stavros Orfanoudakis, Nathan Ordóñez Cardenas, Juan S Giraldo, and Pedro P Vergara.
532 Powerflownet: Power flow approximation using message passing graph neural networks. *Inter-
533 national Journal of Electrical Power & Energy Systems*, 160:110112, 2024.

534

535 Tania B Lopez-Garcia and José A Domínguez-Navarro. Power flow analysis via typed graph neural
536 networks. *Engineering Applications of Artificial Intelligence*, 117:105567, 2023.

537

538 David Mhlanga. Artificial intelligence and machine learning for energy consumption and production
539 in emerging markets: a review. *Energies*, 16(2):745, 2023.

540

541 Christopher Morris, Martin Ritzert, Matthias Fey, William L Hamilton, Jan Eric Lenssen, Gaurav
542 Rattan, and Martin Grohe. Weisfeiler and leman go neural: Higher-order graph neural networks.
543 In *Proceedings of the AAAI conference on artificial intelligence*, volume 33, pp. 4602–4609, 2019.

540 Rahul Nellikkath and Spyros Chatzivasileiadis. Physics-informed neural networks for ac optimal
541 power flow. *Electric Power Systems Research*, 212:108412, 2022.
542

543 Quang-Ha Ngo, Bang LH Nguyen, Tuyen V Vu, Jianhua Zhang, and Tuan Ngo. Physics-informed
544 graphical neural network for power system state estimation. *Applied Energy*, 358:122602, 2024.
545

546 Damian Owerko, Fernando Gama, and Alejandro Ribeiro. Optimal power flow using graph neural
547 networks. In *ICASSP 2020-2020 IEEE International Conference on Acoustics, Speech and Signal
548 Processing (ICASSP)*, pp. 5930–5934. IEEE, 2020.
549

550 Antonio Trias. The holomorphic embedding load flow method. In *2012 IEEE Power and Energy
551 Society General Meeting*, pp. 1–8. IEEE, 2012.
552

553 Anna Varbella, Kenza Amara, Blazhe Gjorgiev, and Giovanni Sansavini. Powergraph: A power
554 grid benchmark dataset for graph neural networks. *Advances in neural information processing
555 systems*, 2024.
556

557 Petar Veličković, Guillem Cucurull, Arantxa Casanova, Adriana Romero, Pietro Lio, and Yoshua
558 Bengio. Graph attention networks. In *International Conference on Learning Representations
559 (ICLR)*, 2018.
560

561 Zonghan Wu, Shirui Pan, Fengwen Chen, Guodong Long, Chengqi Zhang, and S Yu Philip. A
562 comprehensive survey on graph neural networks. *IEEE Transactions on neural networks and
563 learning systems*, 32(1):4–24, 2020.
564

565 Ziwei Zhang, Peng Cui, and Wenwu Zhu. Deep learning on graphs: A survey. *IEEE Transactions
566 on Knowledge and Data Engineering*, 34(1):249–270, 2020.
567

568 Ray Daniel Zimmerman, Carlos Edmundo Murillo-Sánchez, and Robert John Thomas. Matpower:
569 Steady-state operations, planning, and analysis tools for power systems research and education.
570 *IEEE Transactions on power systems*, 26(1):12–19, 2010.
571

572

573

574

575

576

577

578

579

580

581

582

583

584

585

586

587

588

589

590

591

592

593